J. Fluid Mech. (2003), *vol.* 484, *pp.* 303–327. © 2003 Cambridge University Press
DOI: 10.1017/S0022112003004385 Printed in the United Kingdom

Flow rate and electric current emitted by a Taylor cone

By F. J. HIGUERA

ETS Ingenieros Aeronáuticos, Plaza Cardenal Cisneros 3, 28040 Madrid, Spain

(Received 11 March 2002 and in revised form 21 January 2003)

Under certain conditions, the free surface of a conducting liquid subject to an electric field elongates into a cone whose apex emits a thin stationary jet that carries an electric current. The structure of the flow in the cone-to-jet transition region is investigated here, assuming that the size of this region is small compared with any other length of the system where the conical meniscus is formed. The local problem depends then on three non-dimensional parameters, two of which are properties of the liquid while the third measures the flow rate injected through the meniscus. Numerical solutions are computed and the electric current is determined as a function of these parameters. A qualitative asymptotic analysis of the physically important limit of large non-dimensional flow rates gives an electric current increasing as the square root of the flow rate and independent of the dielectric constant of the liquid. When the inertia of the liquid is taken into account, the flow in this asymptotic limit is effectively inviscid in the bulk of the transition region, where the electric current is dominated by conduction in the liquid and the surface is close to an equipotential of the electric field in the gas. The effects of the viscosity of the liquid, the current transported by convection of the surface charge, and the electric shear at the surface come into play in a slender region of the jet. The limit of small non-dimensional flow rates is briefly discussed.

1. Introduction

When the meniscus of an electrically conducting liquid is subject to an electric field, electric charge is induced at the surface of the liquid and an electric stress appears that stretches the meniscus in the direction of the field. If the electric field is sufficiently strong and liquid is continuously supplied, then the meniscus becomes a cone whose apex may either pulsate and shed charged drops or emit a thin stationary jet that breaks into charged drops only at some distance downstream of the cone. This phenomenon is the basis of a number of applications in different fields (Bailey 1988; Grace & Marijnissen 1994). The second regime, termed the cone–jet regime by Cloupeau & Prunet-Foch (1989), is of special interest in the generation of monodisperse sprays of ultrafine drops, the size of which can be controlled in the micrometer to nanometer range mainly by varying the injected flow rate and the electrical conductivity of the liquid. Other applications include mass spectrometry of macromolecules (Fenn *et al.* 1989; Smith *et al.* 1991) and space thrusters (Martínez-Sánchez *et al.* 1999; Mueller 2000, and references therein). Loscertales *et al.* (2002) discuss a recent application to the generation of capsules.

Analysis of these flows began with the pioneering works of Zeleny (1914, 1915, 1917) and Vonnegut & Neubauer (1952), while Taylor (1964) explained the hydrostatic

https://doi.org/10.1017/S0022112003004385 Published online by Cambridge University Press

equilibrium of surface tension and electric stress responsible for the conical meniscus in the absence of motion. Further work aimed at determining the electric current and the size of the drops as functions of the flow rate, the properties of the liquid and the conditions of the experiments, as well as to clarify the forces driving the flow and the different modes of operation of an electrospray, was carried out by Jones & Thong (1971), Mutoh, Kaieda & Kamimura (1979), Smith (1986), Hayati, Bailey & Tadros (1986, 1987*a*, *b*), Cloupeau & Prunet-Foch (1989, 1990, 1994), Gomez & Tang (1994) and Chen, Pui & Kaufman (1995), among others. Fernández de la Mora (1992) proposed a model of the spray in which the drops occupy a cone whose apex coincides with that of the meniscus and found that, in agreement with experiments with flow-injecting menisci, the angle of the meniscus is not a constant but depends on the angle of the spray when the space charge of the drops is taken into account. Lagrangian models have been developed by Gañán-Calvo *et al.* (1994*b*) and Hartman *et al.* (1999) to follow the drops of the spray. Mestel (1994) discusses two models of high-Reynolds-number recirculating flows in conical menisci, one of which allows for angles different from the Taylor angle.

The experimental and theoretical investigation of the mechanics of the flow with the purpose of finding scaling laws of the current and size of the drops emitted by a Taylor cone was initiated by Fernández de la Mora *et al.* (1990), whose inertial scaling of the radius of the jet fits numerous data in the literature. Working with liquids of high electrical conductivity to minimize the influence of the surrounding electrostatic environment, Fernández de la Mora & Loscertales (1994) find a square-root dependence of the electric current on the flow rate, which they explain theoretically by considering the sink flow established in the conical meniscus by the injected flow rate and estimating the electric current as that due to the convection of the equilibrium surface charge of the Taylor solution by the sink flow in a relaxation region around the apex where electric relaxation ceases to be able to maintain the equilibrium of surface charge. This happens because the residence time of the flow in the relaxation region is of the order of the electric relaxation time, a property of the liquid equal to the ratio of its permittivity to its electrical conductivity. In addition, and in agreement with their experimental results, these authors take the size of the relaxation region as an estimate of the size of the drops.

Building on the work of Fernández de la Mora and coworkers, Gañán-Calvo, Dávila & Barrero (1994*a*, 1997) focus on the flow in the jet and assume that the surface charge is in equilibrium, in the sense that the electric displacement in the liquid is small compared with the electric displacement in the gas. These authors propose that, for liquids with high conductivity and viscosity, the electric current and the size of the drops should scale with the current and the radius of the jet in a region whose length they estimate from their conservation equations specialized for one-dimensional flow. They also propose alternative scaling laws for liquids with low conductivity and viscosity. Somewhat different laws are derived by Gañán-Calvo (1997) on the basis of a consistent calculation of the asymptotic structure of the jet far downstream of the cone and an analytic solution for the shape of the upstream cone modified by the presence of the electric charge of the jet.

Although differing in other important aspects, which include basic elements of their theoretical models and their predictions of the drop size, Fernández de la Mora & Loscertales (1994), Gañán-Calvo *et al.* (1994*a*, 1997) and Gañán-Calvo (1997) agree that the electric current increases as the square root of the flow rate, at least in some ranges of operation of the electrospray. An experimental investigation comparing the predictions of the first two works was carried out by Chen & Pui (1997). More

https://doi.org/10.1017/S0022112003004385 Published online by Cambridge University Press

recently, Gamero-Castaño & Hruby (2002) have used time-of-flight and stopping-potential techniques to elucidate a number of characteristics of electrosprays of tributyl phosphate solutions, such as the velocity and electric potential of the liquid at the breakup point of the jet, and some properties of the breakup process and of the drops. These authors find that, within the existing uncertainties, their measured radius of the jet at breakup may fit the predictions of Fernández de la Mora & Loscertales (1994) as well as those of Gañán-Calvo (1997), and thus they cannot be used to decide between the two competing theories, though the agreement is slightly better with the latter than with the former.

The structure of the cone–jet has been analysed by Cherney (1999*a*, *b*) in the asymptotic limit of small flow rates. This author concludes that the square-root relation between the current and the flow rate should hold in this limit also. Another result of his analysis is that the transition region where the meniscus departs significantly from a Taylor cone coincides with the relaxation region of Fernández de la Mora & Loscertales (1994), and that the creeping flow of the liquid in this region is the superposition of a recirculating flow induced by the electric shear at the surface, which is no longer an equipotential, and the sink flow used in the estimates of Fernández de la Mora & Loscertales. A formal inconsistency of the analysis is that a certain capillary number which should tend to zero as the cubic root of the flow rate is assumed to be of order unity. When this is fixed, only the pressure variations and viscous stresses of the recirculating flow contribute to deform the surface in the transition region of Cherney's analysis. But the recirculating flow alone cannot generate a jet and, in addition, being stronger than the sink flow in Fernández de la Mora & Loscertales (1994), it would make the residence time small compared with the electric relaxation time long before reaching the transition region.

This paper is devoted to an analysis of the cone-to-jet transition region in the stationary cone–jet regime of electrospraying. In electrospraying experiments, the meniscus is typically held at the end of a metallic capillary which is fed with the desired flow rate and set at a high voltage relative to a ground collecting electrode at some distance from the meniscus. In many cases, the radius of the electrically charged jet issuing from the transition region around the tip of the meniscus is small compared with the radius of the capillary and the length of the jet (from inception to breakup). This condition allows an idealized problem to be posited in which the transition region is small compared with any other length of the system, be this the radius of the capillary, the distance to jet breakup, or the interelectrode distance. All such lengths become irrelevant to the local problem. The voltage applied between the electrodes is the ultimate cause of the electric field seen by the transition region, but this field is modified by the charge of the spray in the space between the jet and the far electrode and, to a lesser extent, by the adjustment of the meniscus between the rim of the capillary and the transition region. In addition, the field is intensified locally by the very existence of the conical meniscus. All these effects make the electric field around the transition region largely independent of the details of any particular experimental configuration. In fact, it will be seen in § 2 that the electric field in an intermediate region large compared with the transition region but still small compared with any other length coincides in first approximation with the electric field of the Taylor (1964) solution.

A non-dimensional problem for the transition region is formulated in § 2, whose solution depends on three non-dimensional parameters, two of which are properties of the liquid while the third is the non-dimensional flow rate injected through the meniscus. The numerical solution of this problem for different values of the three

https://doi.org/10.1017/S0022112003004385 Published online by Cambridge University Press

parameters is presented in § 3, followed by a qualitative description of the asymptotic structure of the solution for large values of the non-dimensional flow rate. This analysis gives an electric current increasing as the square root of the flow rate and asymptotically independent of the dielectric constant of the liquid, both when the inertia of the liquid has importance and when it is negligible, though a number of different double limits can be distinguished in the second case if the flow rate and the dielectric constant are both large. The case of small non-dimensional flow rates and the existence of a minimum flow rate below which a stationary cone–jet cannot be established are discussed briefly.

2. Formulation

Consider first the Taylor (1964) cone. The surface of an electrically conducting liquid in equilibrium is an equipotential of the electric field, and this field induces a surface electric charge that screens the liquid from the electric field in the gas. The hydrostatic balance of surface tension and normal electric stress at the conical surface of the liquid is $\gamma/R\tan\alpha = \frac{1}{2}\epsilon_0 E_n^2$, where γ is the surface tension of the liquid, α and R are the semiangle of the cone and the distance from its apex, ϵ_0 is the permittivity of vacuum, and E_n is the electric field in the gas, which is normal to the surface. This balance requires $E_n = (2\gamma/\epsilon_0 R\tan\alpha)^{1/2}$, and the density of free surface charge in equilibrium is $\sigma = \epsilon_0 E_n$. Writing $\boldsymbol{E} = \nabla\varphi$ in the gas, where φ, the negative of the electric potential, is a harmonic function regular outside the cone, such a surface field amounts to $\varphi = AR^{1/2}P_{1/2}(\cos\theta)$. Here $P_{1/2}$ is Legendre's function of degree $1/2$, θ is the angle around the apex measured from the prolongation of the axis of the cone, which is the surface $\theta = \pi - \alpha$, and

$$A = \left(\frac{2\gamma}{\epsilon_0 P_{1/2}'^2(-\cos\alpha)\sin^2\alpha\tan\alpha}\right)^{1/2}.$$

In addition, the condition that the cone should be an equipotential of the electric field ($\varphi(R, \pi - \alpha) = 0$) requires that $\cos(\pi - \alpha)$ be the first zero of $P_{1/2}$, i.e. that $\alpha \approx 49.29°$. The hydrostatic balance in Taylor's solution thus determines the angle of the cone and the strength of the electric field around the cone, measured by A. This means that, for a given configuration of the electrodes creating the electric field and a given pressure at the inlet of the capillary holding the meniscus (or a given volume of liquid), the solution will be realized only for a particular value of the voltage applied between the electrodes. Such a voltage has been computed by Pantano, Gañán-Calvo & Barrero (1994) for a needle–plate geometry. Equilibrium solutions with smooth surfaces that tend to a cone only far from its apparent apex, or no equilibrium solution at all, should be expected for other values of the voltage.

If liquid is injected through the capillary, then, in a certain range of voltages and flow rates corresponding to the so-called cone–jet regime, the liquid leaves the meniscus as a jet that emanates from an axisymmetric cone-to-jet transition region around the apex of the cone, as in the sketch of figure 1. The jet may extend a large distance downstream of the transition region before it breaks up into charged drops. An electric current accompanies this flow, both because the free electric charge at the surface is convected by the flow and because an electric field and its associated ohmic conduction current appear in the liquid. There is no net charge in the bulk of the liquid and the mobility of the surface charge will be neglected. The bulk conduction current dominates in the meniscus far upstream of the transition region, where the speed of the liquid and the surface charge density are small and the cross-section of

https://doi.org/10.1017/S0022112003004385 Published online by Cambridge University Press

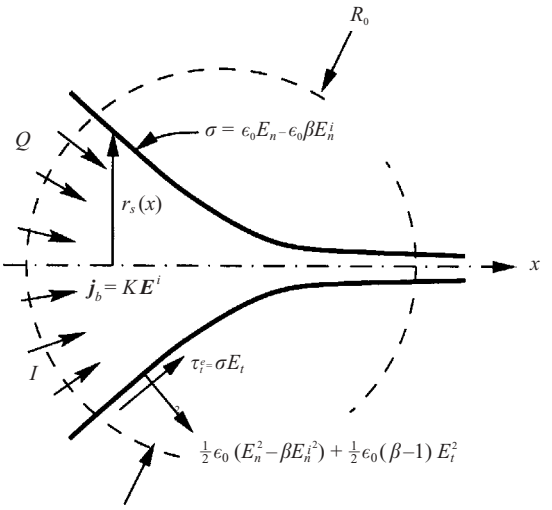


FIGURE 1. Definition sketch.

the meniscus is large. The surface convection current begins to become important when these conditions change in the transition region and beyond, and eventually it dominates over the conduction current and is the only transport mechanism left when the jet breaks into drops. The conservation equation for the free surface charge is

$$\frac{\mathrm{d}I_s}{\mathrm{d}x} = 2\pi r_s K E_n^i \left(1 + r_s'^2\right)^{1/2} \quad \text{with} \quad I_s = 2\pi r_s v_s \sigma, \tag{2.1}$$

where x is the distance along the symmetry axis, $r_s(x)$ and $v_s(x)$ are the radius of the surface cross-section and the velocity of the liquid at the surface, K is the electrical conductivity of the liquid, and E_n^i is the component of the electric field normal to the surface at the liquid side. The surface charge density σ is given by

$$\sigma = \epsilon_0 \left(E_n - \beta E_n^i\right) \tag{2.2}$$

in terms of the normal components of the electric field at the gas and liquid sides of the surface and the dielectric constant of the liquid β (Landau & Lifshitz 1960). Hereafter the superscript i denotes the electric field and the negative of the electric potential in the liquid ($\boldsymbol{E}^i = \nabla\varphi^i$), while no superscript is used to denote these magnitudes in the gas. The right-hand side of (2.1) is the conduction-to-convection charge transfer rate, due to the component of the conduction current density ($\boldsymbol{j}_b = K\boldsymbol{E}^i$) normal to the surface. Since the charge conservation equation in the bulk of the liquid reduces to $\nabla\cdot\boldsymbol{j}_b = 0$ in the absence of bulk charge, equation (2.1) establishes that the sum of the convection and conduction currents across a section of the meniscus, $I_s(x)$ and $I_b(x) = 2\pi K \int_0^{r_s} E_x^i r\,\mathrm{d}r$, respectively, where r is the distance to the symmetry axis, is a constant, equal to the total current I transported by the liquid. Notice also that $\nabla\cdot\boldsymbol{j}_b = 0$ becomes $\nabla^2\varphi^i = 0$ for a constant-conductivity liquid, in which case the electric potentials are harmonic functions in both phases.

The components of the electric stress normal and tangent to the surface, τ_n^e and τ_t^e respectively, are written here for reference (Landau & Lifshitz 1960):

$$\tau_n^e = \tfrac{1}{2}\epsilon_0 \left(E_n^2 - \beta E_n^{i^2}\right) + \tfrac{1}{2}\epsilon_0(\beta - 1)E_t^2, \quad \tau_t^e = \sigma E_t, \tag{2.3}$$

https://doi.org/10.1017/S0022112003004385 Published online by Cambridge University Press

where E_t is the component of the electric field tangent to the surface, which is continuous across the surface. See figure 1.

Scales for the variables in the cone-to-jet transition region, the analysis of which is the subject of this paper, can be worked out as follows. The transition region is small compared with the meniscus in the conditions envisaged here. Let Q_0 be a characteristic flow rate, to be determined below. The scales of the size of the transition region, R_0 say, and the velocity of the liquid in it, $v_0 = Q_0/R_0^2$, come from the condition that the pressure variation due to the motion of the liquid should be of the same order as the surface tension force in order for the surface to depart from a Taylor cone. Assuming that the inertia of the liquid is important, so that $\Delta\ p = O(\rho v_0^2)$, this order-of-magnitude balance ($\rho v_0^2 = \gamma/R_0$) gives $R_0 = (\rho Q_0^2/\gamma)^{1/3}$, which is the inertial scale of Fernández de la Mora *et al.* (1990). The condition that the electric stress at the surface should also be included then gives the scale of the electric field $E_0 = (\gamma/\epsilon_0 R_0)^{1/2}$, and the scales of the electric potential and the charge density are $\varphi_0 = E_0 R_0$ and $\sigma_0 = \epsilon_0 E_0$. In the same manner, the scales of the surface and bulk currents that follow from their definitions with numerical factors omitted are $R_0 v_0 \sigma_0$ and $K E_0 R_0^2$, respectively. But these two variables should be of the same order if the bulk current becomes surface current in the transition region with $I = I_s + I_b$ constant. The condition $R_0 v_0 \sigma_0 = K E_0 R_0^2$ determines $Q_0 = \epsilon_0 \gamma/\rho K$ and thus all the other scales. Summarizing,

$$\left.\begin{gathered} Q_0 = \frac{\epsilon_0 \gamma}{\rho K}, \quad R_0 = \left(\frac{\epsilon_0^2 \gamma}{\rho K^2}\right)^{1/3}, \quad v_0 = \left(\frac{\gamma K}{\rho \epsilon_0}\right)^{1/3}, \\ E_0 = \left(\frac{\rho^{1/2} \gamma K}{\epsilon_0^{5/2}}\right)^{1/3}, \quad I_0 = \frac{\epsilon_0^{1/2} \gamma}{\rho^{1/2}}, \quad \varphi_0 = E_0 R_0, \quad \sigma_0 = \epsilon_0 E_0, \end{gathered}\right\} \tag{2.4}$$

where I_0 is the common value of the two electric current scales. Scales (2.4) were first introduced by Gañán-Calvo *et al.* (1994*a*, 1997) using dimensional analysis.

As an example, the values of R_0 for the highest conductivity solution of 1-octanol and the lowest conductivity solution of water in the experiments of Fernández de la Mora & Loscertales (1994) are 1.67×10^{-8} m and 1.07×10^{-7} m, respectively, and the values of Q_0 are 1.22×10^{-14} m^3 s^{-1} and 2.99×10^{-13} m^3 s^{-1} for these two solutions. The small values of R_0 are typical of many experiments, which justifies the assumption of a transition region small compared with any other length of the system. More precise estimates can be obtained by noticing that the actual size of the transition region scaled with R_0 increases proportionally to the 2/3 power of the flow rate scaled with Q_0 (from the pressure–surface tension balance in the preceding paragraph with Q_0 replaced by a generic flow rate; see also § 3.2 below). According to this estimate, flow rates of order $Q_0(D_c/R_0)^{3/2}$ would be needed for the size of the transition region to become of the order of the diameter of the capillary D_c. With D_c in the order of 1 mm, these flow rates are over a million times Q_0, much larger than the flow rates typical of the cone–jet regime.

The last condition above, giving Q_0 and closing the sequence, deserves some comments. Equation (2.1) states that the bulk-to-surface current transfer causes the variation of I_s with x. Since $\mathrm{d}I_s/\mathrm{d}x = O(v_0 \epsilon_0 E_0)$ in the transition region (using $\sigma_0 = \epsilon_0 E_0$ and the fact that both x and r_s scale as R_0 in the non-slender transition region), the balance of the two terms of (2.1) implies

$$E_n^i = O\left(\frac{\epsilon_0 E_0 v_0}{K\ R_0}\right) = O\left(\frac{E_0}{\beta}\frac{t_e}{t_r}\right),$$

https://doi.org/10.1017/S0022112003004385 Published online by Cambridge University Press

where $t_r = R_0/v_0$ is the residence time of the liquid in the transition region and $t_e = \epsilon_0\beta/K$ (a property of the liquid only) is the electric relaxation time brought about by the charge transfer process. If $t_r \gg t_e$, then charge transfer is able to balance the variations of surface charge with only a small electric field $E_n^i \ll E_0/\beta$ in the liquid, or, in other words, the surface charge is screening the liquid from the electric field in the gas, as in the absence of motion. On the contrary, if $t_r \ll t_e$, then $E_n^i \gg E_0/\beta$ would be required, which is not available because there is no mechanism that could create an electric displacement $\epsilon_0\beta E^i$ in the liquid large compared with the electric displacement $\epsilon_0 E$ in the gas (see (2.2), where $E_n^i = E_n/\beta$ at most, when $\sigma = 0$). Thus the right-hand side of (2.1) is negligible in this case, and the surface current should be nearly independent of x. This is a difficult condition to impose because σ, r_s and v_s are already constrained by (2.2) and the other conservation equations (see below). In fact the condition $t_r \ll t_e$ is never realized experimentally (Gañán-Calvo *et al.* 1997); the cone–jet regime ends before the residence time t_r becomes small compared with the electric relaxation time, giving way to other non-stationary regimes (see Cloupeau & Prunet-Foch 1994 and Jaworek & Krupa 1999 for classifications of the possible regimes). Up to a factor of β, the condition $t_r = t_e$ is equivalent to the condition used before to determine Q_0. Fernández de la Mora & Loscertales (1994) propose that the condition $t_r = t_e$ should be always satisfied, irrespective of the flow rate, in a certain relaxation region that has been described in the introduction. They use this condition to determine the order of the electric current as a function of the flow rate. On the other hand, Gañán-Calvo *et al.* (1994*a*) argue that, since the residence time increases with the flow rate ($t_r = R/v = \rho Q/\gamma$ using the inertial scales in the paragraph above (2.4) for a generic flow rate), Q_0 should be characterizing the minimum flow rate compatible with the cone–jet regime, and $t_r \gg t_e$ everywhere for higher flow rates.

There is yet another feature of the scales (2.4) that is worth noticing. The electric shear on the surface is σE_t (see (2.3)), where the component of the electric field tangent to the surface is of the order of E_0 in the transition region when $t_r = t_e$, again up to a factor of β. Provided that the Reynolds number defined in (2.8) below is of order unity, which is the case for many liquids, this electric shear is of order $\mu v_0/R_0$, where μ is the viscosity of the liquid, and thus plays an important role in pulling the liquid in the transition region out of the meniscus (Smith 1986; Hayati *et al.* 1987*a*).

The scales (2.4) are used in what follows to non-dimensionalize the problem, denoting the non-dimensional variables with the same symbols used before for their dimensional counterparts. Neglecting the pressure variations and viscous stresses of the gas on the surface of the liquid, the non-dimensional governing equations and boundary conditions at the surface are

$$\nabla\cdot\boldsymbol{v} = 0, \quad \boldsymbol{v}\cdot\nabla\boldsymbol{v} = -\nabla p + \frac{1}{Re}\nabla^2\boldsymbol{v}, \quad \nabla^2\varphi^i = 0 \quad \text{for} \quad r < r_s(x), \tag{2.5a–c}$$

$$\nabla^2\varphi = 0 \quad \text{for} \quad r > r_s(x) \tag{2.6}$$

and

$$r = r_s : \begin{cases} \nabla\cdot\boldsymbol{n} = p - \boldsymbol{n}\cdot\boldsymbol{\tau}'\cdot\boldsymbol{n} + \frac{1}{2}\left(E_n^2 - \beta E_n^{i^2}\right) + \frac{1}{2}(\beta-1)E_t^2, & (2.7a) \\ \boldsymbol{t}\cdot\boldsymbol{\tau}'\cdot\boldsymbol{n} = \sigma E_t, & (2.7b) \\ \dfrac{\mathrm{d}}{\mathrm{d}x}(r_s v_s \sigma) = r_s E_n^i\left(1 + r_s'^2\right)^{1/2}, & (2.7c) \\ \sigma = E_n - \beta E_n^i, \qquad \boldsymbol{v}\cdot\boldsymbol{n} = 0, \qquad \boldsymbol{E}\cdot\boldsymbol{t} = \boldsymbol{E}^i\cdot\boldsymbol{t}, & (2.7d–f) \end{cases}$$

https://doi.org/10.1017/S0022112003004385 Published online by Cambridge University Press

where (x, r) are cylindrical coordinates; $\boldsymbol{n} = (-r_s', 1)/(1 + r_s'^2)^{1/2}$ and $\boldsymbol{t} = (1, r_s')/(1 + r_s'^2)^{1/2}$, with $r_s' = \mathrm{d}r_s/\mathrm{d}x$, are unit normal and tangent vectors at the surface; $E_n = \boldsymbol{E}\cdot\boldsymbol{n}$ and $E_t = \boldsymbol{E}\cdot\boldsymbol{t}$, and similarly for the electric field in the liquid; $v_s = \boldsymbol{v}\cdot\boldsymbol{t}$, where $\boldsymbol{v}$ is the velocity of the liquid, and $\boldsymbol{\tau}' = (2Re)^{-1}[\nabla\boldsymbol{v} + (\nabla\boldsymbol{v})^T]$ is the viscous stress tensor. Equations (2.7*a*) and (2.7*b*) are the balances of stresses normal and tangent to the surface, where p is the excess of pressure of the liquid above the gas pressure, non-dimensionalized with ρv_0^2, and the electric stresses (2.3) have been rewritten in non-dimensional variables. The non-dimensional parameters appearing in these equations are

$$\beta \quad \text{and} \quad Re = \frac{\rho^{1/3}\epsilon_0^{1/3}\gamma^{2/3}}{\mu K^{1/3}}, \tag{2.8}$$

which are both properties of the liquid. The second parameter is $Re = \rho v_0 R_0/\mu$ and thus measures the relative importance of inertia to viscous forces when the non-dimensional variables are of order unity.

Far-field boundary conditions are needed to complete the formulation of the problem. Assuming that a conical spray of charged drops issues from the apex of the conical meniscus, Fernández de la Mora (1992) demonstrated that the field of the space charge carried by the drops of the spray depends of the distance to the apex with the same $R^{-1/2}$ law as the field of the surface charge of a Taylor cone, and that the combination of the two fields leads to conical menisci with angles different from the Taylor angle α. In the situation envisaged here, however, the breakup of the jet into drops and the dispersion of the drops into a spray are processes that occur only very far downstream of the transition region, so that the results of Fernández de la Mora (1992) would be applicable even further if at all. Far-field boundary conditions for the problem in the transition region should come from the analysis of an intermediate region around the transition region, of size large compared with R_0 ($R = |\boldsymbol{x}| \gg 1$ in non-dimensional variables) but still small compared to the total length of the jet. The only electric charge present in this region is on the surfaces of the meniscus and the jet; the space charge in the far spray has only a global screening effect equivalent to that of changing the voltage applied between the electrodes to an effective value smaller than the real voltage. Consider the meniscus in this intermediate region. Assuming that the surface will tend to a cone far upstream of the transition region, the electric field in the liquid should decay as I/R^2 to keep a constant electric current I, and the velocity also decays sufficiently rapidly (actually as $R^{-3/2}$ due to the electric shear on the surface; see Barrero *et al.* 1999 and below) for the normal stress of the liquid on the surface to become small compared with the normal stress due to the surface tension when $R \to \infty$. Thus we are left in this far region with the surface tension–normal electric stress balance characteristic of Taylor's solution, which requires $E_n = O(R^{-1/2})$. This electric field is large compared with the $O(I/R^2)$ field in the liquid, so that the surface is effectively an equipotential ($E_t \ll E_n$) despite the presence of an electric current in the liquid. Moreover, the electric field induced by the charge at the surface of the jet far downstream of the transition region decays faster than $R^{-1/2}$ away from the jet, as will be seen in the next two paragraphs (but see also § 3.3), and thus the leading-order solution for the gas-phase electric potential when $R \to \infty$ coincides with Taylor's solution $\varphi_T = AR^{1/2}P_{1/2}(\cos\theta)$, with $A = [2/P_{1/2}'^2(-\cos\alpha)\sin^2\alpha\tan\alpha]^{1/2} = 1.3459\ldots$ in non-dimensional variables. The angle of the meniscus tends to the Taylor angle α.

The flow and charge distribution in the jet far downstream of the transition region can now be estimated following the original analysis of Gañán-Calvo (1997). The

https://doi.org/10.1017/S0022112003004385 Published online by Cambridge University Press

following order-of-magnitude relations between the characteristic values of the non-dimensional variables hold in the jet for $x \to \infty$:

$$vr_s^2 \sim Q, \quad \sigma v r_s \sim I, \quad \frac{v^2 r_s^2}{x} \sim \sigma E_t r_s, \quad E_t \sim \frac{1}{x^{1/2}}. \tag{2.9}$$

The first two balances express the conservation of mass (Q is the flow rate non-dimensionalized with Q_0) and electric current, which is mainly surface current in the jet. The third balance comes from the axial component of the momentum equation (2.5*b*) integrated across the jet which, upon using (2.7*b*) and neglecting viscous stresses associated with the x-derivatives of the velocity, is $\mathrm{d}[\pi r_s^2(v^2 + p)]/\mathrm{d}x = 2\pi r_s \sigma E_t$ in the far jet. Finally, the fourth condition (2.9) expresses that the field tangent to the surface is dominated by the contribution of the cone, as mentioned before. These four relations yield (Gañán-Calvo 1997)

$$r_s = O\left(\frac{Q^{3/4}/I^{1/4}}{x^{1/8}}\right), \quad v = O\left(\frac{I^{1/2}}{Q^{1/2}} x^{1/4}\right), \quad \sigma = O\left(\frac{I^{3/4}/Q^{1/4}}{x^{1/8}}\right) \tag{2.10}$$

for $x \to \infty$. The electric field normal to the surface of the jet is $E_n = \sigma \gg E_t$ from (2.7*d*). Unlike E_t, the normal field is due to the local charge in the jet. The contribution of the normal electric stress to (2.7*a*), of the order of E_n^2, is negligible compared with the contribution of the surface tension, of order $1/r_s$. The surface tension is balanced by a pressure variation of order $1/r_s$, which, however, is small compared with the dynamic pressure of the liquid. This means that the acceleration of the jet under the action of the surface electric shear occurs effectively at constant pressure.

The field induced by the charge of the jet far downstream of the cone can be estimated by noticing that, from the point of view of the gas, the charged jet acts as a line distribution of charge of strength $\Phi = O(\sigma r_s)$. The axial component of the field of this distribution is $(2\pi)^{-1} \ln(r/x)\, \mathrm{d}\Phi/\mathrm{d}x = O(Q^{1/2} I^{1/2}/R^{5/4})$ at leading order for $x = O(R) \gg 1$, up to logarithms, and this is also the order of the whole field induced by the far jet at distances of $O(R)$ from its surface (Ashley & Landahl 1965). This is a small field compared with the $O(R^{-1/2})$ field of Taylor's solution, and leads to a small perturbation $\varphi_1 = O(Q^{1/2} I^{1/2}/R^{1/4})$ to the electric potential in the gas for $R \to \infty$. The condition that $\varphi_T + \varphi_1 = 0$ at the surface of the meniscus, $\theta = \pi - \alpha - \delta(R)$ say, determines the small departure of the surface from a Taylor cone: $\delta(R) = O(Q^{1/2} I^{1/2}/R^{3/4})$.

The far-field boundary conditions for (2.5) and (2.6) can be summarized as follows:

$$\varphi = \varphi_T(R, \theta) + O\left(\frac{Q^{1/2} I^{1/2}}{R^{1/4}}\right) \tag{2.11}$$

in the gas, and

$$\left.\begin{aligned} \varphi^i &= \frac{I}{2\pi(1 - \cos\alpha)R}, \\ \psi &= -\frac{A\, P'_{1/2}(-\cos\alpha)}{2\pi(1 - \cos\alpha)} I Re R^{1/2} f_B(-\cos\theta) + \frac{Q}{2\pi(1 - \cos\alpha)}(1 + \cos\theta), \\ \omega &\to 0 \end{aligned}\right\} \tag{2.12}$$

in the meniscus, where ψ and ω are the stream function and the vorticity. The first term of ψ accounts for the recirculating flow induced by the electric shear on the meniscus (Barrero *et al.* 1999) and the second term accounts for the flow rate Q injected through the capillary. The function $f_B(\xi)$, introduced by Barrero *et al.* (1999),

https://doi.org/10.1017/S0022112003004385 Published online by Cambridge University Press

is the solution of

$$(1-\xi^2)\left(f_B^{\mathrm{iv}} - 4\xi f_B''' + \tfrac{3}{2} f_B''\right) - \tfrac{15}{16} f_B = 0,$$
$$f_B(1) = f_B(\cos\alpha) = f_B''(\cos\alpha) + 1 = 0, \quad f_B'(1) < \infty.$$

In addition, $\partial\varphi^i/\partial x = \partial\varphi_T/\partial x$ in the jet, where the other variables follow the power laws (2.10). Finally, the shift invariance of the whole problem is fixed by setting $r_s = -x\tan\alpha + o(1)$ for $x \to -\infty$, which amounts to fixing the origin of the axial distance x.

This completes the formulation of the problem. The solution of (2.5)–(2.7) and (2.10)–(2.12) should determine the electric current I, the velocity and pressure in the liquid, the electric potential in both phases, and the radius and charge density of the surface for given values of β, Re and the non-dimensional flow rate Q. The fact that the solution depends on three non-dimensional parameters, equivalent to β, Re and Q here, was first noted by Fernández de la Mora & Loscertales (1994), who investigated experimentally the dependence of the current and the size of the drops on these parameters; see also Rosell-Llompart & Fernández de la Mora (1994).

In essence, the electric shear acting on the surface of the liquid can speed up any flow rate injected through the capillary, while the electric current is determined by the condition that only surface convection current should be left far downstream. In principle, the electric current could be assigned an arbitrary value if this latter condition were relaxed and some conduction current were allowed in the far jet, as when the jet impinges onto the far electrode. Then (2.10) would need change.

For the numerical treatment, cylindrical coordinates (x, r) and the equivalent vorticity–stream function form of (2.5a,b) were used, and r was replaced by $\eta = r/r_s(x)$, so that the liquid occupies the region $\eta < 1$ and the gas occupies the region $\eta > 1$. The equations were discretized using finite differences and solved by means of a standard pseudotransient iteration that amounts to adding artificial time derivatives to the discretized equations and letting the pseudotransient solution evolve until a stationary state is attained.

Condition (2.11), that the electric potential in the gas far from the transition region coincides with the Taylor potential at leading order, poses a strong restriction on the voltage applied between the electrodes. Leaving aside the effects of the space charge and the adjustment of the meniscus between the rim of the capillary and the transition region, (2.11) would imply that the relative variation of the voltage about the value leading to a hydrostatic Taylor cone is only of order $Q^{1/2}I^{1/2}/L^{3/4}$, where $L \gg 1$ is the interelectrode distance scaled with R_0. This range should widen when the two effects mentioned above are taken into account, but it will still be fairly narrow for any realistic configuration of the electrodes. The result seems to be in line with experimental observations (Jones & Thong 1971; Cloupeau & Prunet-Foch 1989; Tang & Gomez 1994; Chen *et al.* 1995).

3. Results and discussion

3.1. *Numerical results*

Some streamlines of the flow in the liquid are displayed in figure 2 for $\beta = 5$, $Re = 1$ and the two values of the non-dimensional flow rate $Q = 0.27$ and 4.8 (for which the non-dimensional electric current is $I = 1.1$ and 5.0, respectively). Notice the different scales of the two figures; the size of the cone-to-jet transition region increases with Q. As can be seen, recirculation exists in the transition region in figure 2(a), for the

https://doi.org/10.1017/S0022112003004385 Published online by Cambridge University Press

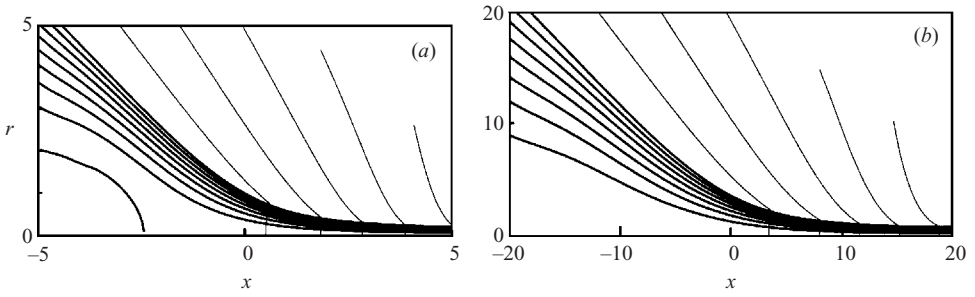


FIGURE 2. Streamlines (thick) and equipotentials of the electric field (thin) for $\beta = 5$, $Re = 1$ and two different flow rates: (*a*) $Q = 0.27$ ($I = 1.1$) and (*b*) $Q = 4.8$ ($I = 5.0$). The outermost streamline of each figure coincides with the surface of the liquid.

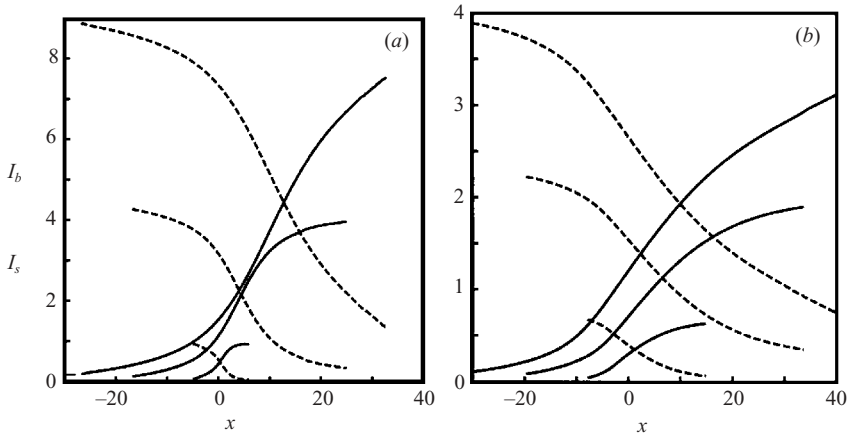


FIGURE 3. Surface convection current (solid) and bulk conduction current (dashed). (*a*) (β, Re) = (5, 1) and $Q = 0.22$, 3.73 and 13.27 (for which $I = 0.99$, 4.32 and 8.89), increasing from bottom to top. (*b*) (β, Re) = (50, 1) and $Q = 0.49$, 3.81 and 9.14 (for which $I = 0.70$, 2.25 and 3.87).

smallest of the two flow rates, but not in figure 2(*b*). The recirculation region becomes more prominent when Q decreases, covering most of the cone and extending into the beginning of the jet for the smallest flow rates for which a numerical solution could be computed. When Q increases, the recirculation region recedes into the cone. This is in line with the asymptotic form of the stream function in (2.12), where, assuming that the ratio Q/I increases with Q, the first term, which represents the recirculating flow induced by the electric shear at the surface, dominates the second term, which is the sink due to the injected flow rate, only when R is large compared with $(Q/I)^2$. Experimental observations of recirculation in the cone were first reported by Hayati *et al.* (1986, 1987*a*). The swirling flow that sometimes accompanies the meridional motion of the liquid has been analysed by Shtern & Barrero (1994, 1995*a*, *b*) and Fernández-Feria *et al.* (1999). The thin curves in figure 2 are equipotentials of the electric field in both phases. The liquid surface tends to an equipotential far upstream, where Taylor's solution applies, but not in the jet, where the electric shear continuously accelerates the flow.

The bulk conduction and surface convection currents are given in figure 3 as functions of the streamwise distance x for $Re = 1$ and different values of β and Q.

https://doi.org/10.1017/S0022112003004385 Published online by Cambridge University Press

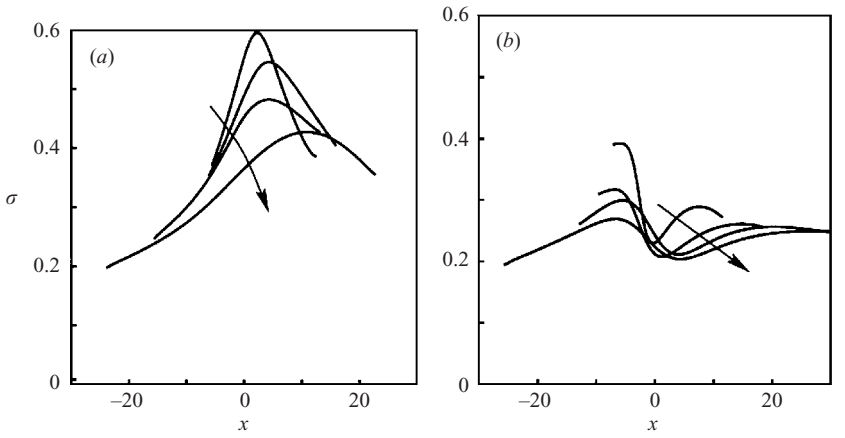


FIGURE 4. Surface charge density. (*a*) $(\beta, Re) = (5, 1)$ and $Q = 0.99$, 2.19, 3.51 and 11.48 (for which $I = 2.17$, 3.34, 4.19 and 8.11), increasing as indicated by the arrow. (*b*) $(\beta, Re) = (50, 1)$ and $Q = 0.56$, 2.07, 3.69 and 6.09 (for which $I = 0.74$, 1.56, 2.23 and 3.02).

The surface current (solid) increases and the bulk current (dashed) decreases with increasing x. The sum of the two currents is the total electric current, which is independent of x and increases with Q. The crossover point at which the surface and bulk currents become equal to each other shifts downstream into the jet with increasing Q, so that the electric current is dominated by bulk conduction in most of the transition region when the non-dimensional flow rate is large. The idea that the surface current becomes important only in the jet was put forward by Gañán-Calvo *et al.* (1994*a*, 1997) and has been used by these authors in subsequent analyses of the jet based on one-dimensional models that take advantage of the slenderness of this region (see, e.g., Gañán-Calvo 1999 and references therein).

Figure 4 shows the surface charge density, $\sigma(x)$, for $Re = 1$ and different values of the flow rate in relatively apolar ($\beta = 5$) and polar ($\beta = 50$) liquids. The charge density varies as $1/|x|^{1/2}$ in the cone upstream of the transition region. For $\beta = 5$, it reaches a maximum in the transition region, where the singularity of Taylor's solution is smoothed out, and decreases in the jet. The maximum charge density decreases with increasing Q because the size of the transition region increases. The position of the maximum shifts downstream into the jet with increasing Q, so that the charge density increases with distance in the leading part of the jet. A characteristic feature of the charge density in figure 4(*b*), for $\beta = 50$, is the fall and rise in the transition region, specially for small values of the flow rate. This local dip is absent from the solutions with $\beta = 5$. It reflects that the electric relaxation time increases with β and the bulk-to-surface charge transfer cannot cope with the fast variation of the surface charge that would be required in the transition region to screen the liquid from the field in the gas. In fact (cf. the discussion following (2.4)), the maximum possible value of the component of the electric field normal to the surface on the liquid side is $E_n^i = E_n/\beta$, from (2.7*d*) with $\sigma = 0$, which can only give $\sigma/E_n = O(t_r/\beta)$ in the transition region (from the balance of the two terms of (2.7*c*)). Thus the charge density cannot satisfy the screening condition $\sigma \approx E_n$ when β increases or the non-dimensional residence time t_r decreases.

Further downstream, the curves of figure 4 for different values of the flow rate begin to coalesce, which makes the charge density nearly independent of the flow rate in the

https://doi.org/10.1017/S0022112003004385 Published online by Cambridge University Press

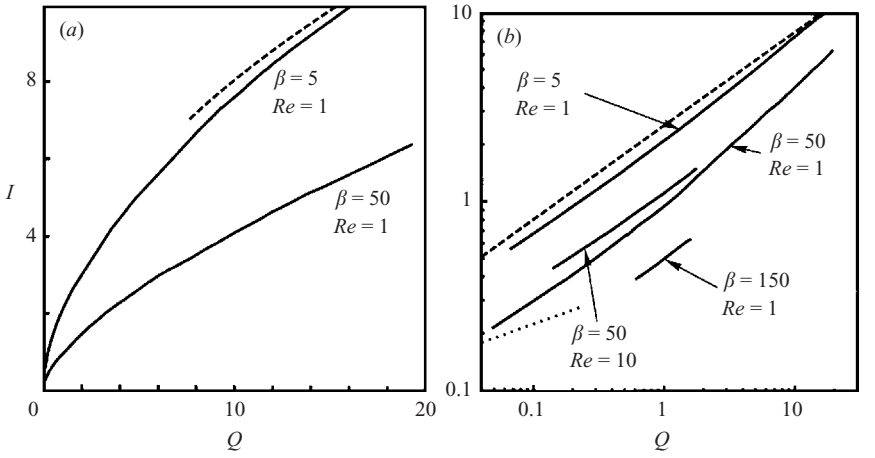


FIGURE 5. Electric current as a function of the flow rate for different values of β and Re. The dashed curve is $I = 2.55\,Q^{1/2}$, from the correlation of experimental data in Gañán-Calvo (1999). The dotted line at the left has slope 1/4. (*b*) Logarithmic representation of (*a*).

region where bulk conduction current becomes surface convection current (around the crossover of figure 3). This feature and a similar coalescence of the curves giving the velocity along the axis of the jet (not displayed) agree with the results obtained by Gañán-Calvo (1999) using a hybrid experimental–numerical technique. Also in agreement with these results is the plateau of the charge density in figure 4(*b*), for $\beta = 50$, in which case it has been possible to extend the computations to values of x somewhat larger than for $\beta = 5$. The charge density should tend to the downstream asymptotic regime (2.10) even further downstream, where the continuous acceleration of the liquid stretches the surface of the jet and leads to a slow decrease of the charge density with streamwise distance. This final regime is clearly not attained within the computational domain used for $\beta = 5$, and in any case the asymptotic variation of σ as $x^{-1/8}$ is probably too slow to be ascertained computationally or experimentally.

The electric current is plotted in figure 5 as a function of the flow rate for different values of β and Re. In all the cases the current increases approximately as the square root of the flow rate in the upper part of the range of the latter variable that has been explored numerically. This is in line with existing experimental results and with scaling laws derived from different theoretical models (Fernández de la Mora & Loscertales 1994; Gañán-Calvo *et al.* 1997; Gañán-Calvo 1997). The logarithmic representation in figure 5(*b*) suggests that the square root is an asymptotic law for high non-dimensional flow rates in the two cases for which the computations have been extended to large values of this variable; namely $(\beta, Re) = (5, 1)$ and $(\beta, Re) = (50, 1)$. (See also the results of § 3.5, which cover a larger range of flow rates.) The dependence of the ratio $I/Q^{1/2}$ on the dielectric constant β for large values of Q is also of interest. The issue has not been settled yet. Results in the literature include $I/Q^{1/2} = f(\beta)/\beta^{1/2}$ with $f(\beta)$ first increasing with β, reaching a plateau and then decreasing slightly (Fernández de la Mora & Loscertales 1994); $f(\beta) \propto \beta^{1/4}$ (Gañán-Calvo *et al.* 1994*a*, 1997); $f(\beta)$ increasing monotonically, first faster than $\beta^{1/4}$ and then slower than $\beta^{1/4}$ (Chen & Pui 1997); and $I/Q^{1/2}$ independent of β (Gañán-Calvo 1997, 1999). This latter result seems at variance with the numerical results in figure 5(*a*) and with existing experimental data for the largest flow rates attainable

https://doi.org/10.1017/S0022112003004385 Published online by Cambridge University Press

in the cone–jet mode. The order-of-magnitude estimates in the following subsection suggest, however, that $I/Q^{1/2}$ asymptotically independent of β could be inescapable for very large values of Q, though this asymptotic result, which requires $Q \gg \beta$ when β is large, may not be easily attained in some practical cases.

3.2. *Estimations for large flow rates*

A qualitative description of the transition region in the asymptotic limit $Q \to \infty$ is proposed in this subsection. The asymptotic structure consists of the transition region proper, which is a non-slender region of effectively inviscid flow where transport of electric current is still dominated by bulk conduction and the liquid surface is nearly an equipotential, followed by a number of slender regions, already in the jet, where surface convection current, viscous forces, and electric shear at the surface come into play, until the flow adjusts to the downstream asymptotic state (2.10).

The size of the non-slender transition region is determined, as in § 2, by the condition that the dynamic pressure of the liquid, whose velocity is of order $v_c = Q/R_c^2$, should be of the order of the normal stress at the surface due to the surface tension, of order $1/R_c$ in non-dimensional variables. This condition gives $R_c = Q^{2/3}$ and $v_c = 1/Q^{1/3}$ for the characteristic non-dimensional size and velocity of the transition region, while the characteristic electric field in the gas is $E_c = 1/Q^{1/3}$, from the condition that the electric stress should also play a role in the balance of normal stresses (2.7*a*).

The flow in the transition region is affected little by viscous forces because

$$\frac{O\left(\boldsymbol{v}\cdot\nabla\boldsymbol{v}\right)}{O\left(Re^{-1}\nabla^2\boldsymbol{v}\right)} = Re\, v_c R_c = Re\, Q^{1/3} \gg 1$$

in the momentum equation (2.5*b*). This means that the flow is not driven by the local electric shear at the surface, which is felt only in a thin surface viscous layer, but by the depression created by the action of the electric shear in the jet far downstream of the transition region. The flow in the transition region is irrotational.

The non-dimensional residence time in the transition region is $t_r = R_c/v_c = Q$, which is large compared with the non-dimensional electric relaxation time $t_e = \beta$ if $Q \gg \beta$, in which case the surface charge screens the liquid from the electric field in the gas and $\sigma \approx E_n$ from (2.7*d*). This result and the estimate of E_n above explain the decrease of the maximum surface charge density in figure 4 with increasing Q.

The surface convection current is $I_s = 2\pi r_s v_s \sigma = O(1)$, independent of Q, while the numerical results show that the total electric current increases with Q. Therefore the electric current in the transition region is dominated by conduction in the bulk of the liquid. On the other hand, the maximum possible conduction current is of the order of $E_c R_c^2 = Q$, if the electric field in the liquid were of the order of E_c. This estimate is very much larger than the observed current, which means that the electric field in the liquid is small compared with E_c and the liquid surface is nearly an equipotential from the point of view of the gas phase.

Rescaling the variables with the characteristic values derived from the foregoing estimates and then letting $Q \to \infty$, we are led to the following problem, where tildes denote rescaled variables:

$$\widetilde{\boldsymbol{v}} = \nabla\widetilde{\phi} \quad \text{with} \quad \nabla^2\widetilde{\phi} = 0 \quad \text{in the liquid } (\widetilde{r} < \widetilde{r}_s(\widetilde{x})), \tag{3.1a}$$

$$\nabla^2\widetilde{\varphi} = 0 \quad \text{in the gas } (\widetilde{r} > \widetilde{r}_s(\widetilde{x})), \tag{3.1b}$$

$$\nabla\cdot\boldsymbol{n} = -\tfrac{1}{2}|\nabla\widetilde{\phi}|^2 + \tfrac{1}{2}|\nabla\widetilde{\varphi}|^2 \quad \text{and} \quad \boldsymbol{n}\cdot\nabla\widetilde{\phi} = \widetilde{\varphi} = 0 \quad \text{at} \quad \widetilde{r} = \widetilde{r}_s(\widetilde{x}), \tag{3.1c}$$

https://doi.org/10.1017/S0022112003004385 Published online by Cambridge University Press

$$\widetilde{\phi} = \frac{1}{2\pi(1-\cos\alpha)\widetilde{R}} \quad \text{for} \quad \widetilde{x} \to -\infty, \tag{3.1d}$$

$$\widetilde{\varphi} = \widetilde{\varphi}_T(\widetilde{R}, \theta) \quad \text{for} \quad \widetilde{R} \to \infty. \tag{3.1e}$$

Here $\widetilde{\phi}$ is the velocity potential rescaled with $v_c R_c$ and $\widetilde{\varphi}_T$ is the electric potential of the Taylor solution in rescaled variables. The electric potential in the liquid rescaled with I/R_c (where the electric current is still unknown) coincides with the velocity potential $\widetilde{\phi}$ because both variables satisfy the same equation and boundary conditions, including the condition $\boldsymbol{n}\cdot\nabla\widetilde{\varphi}^i = 0$ at the surface, which expresses that the bulk-to-surface current transfer rate is negligible in the present region.

When $\widetilde{x} \to \infty$ (or $x \gg Q^{2/3}$), the surface is observed to become a jet with radius decreasing continuously with downstream distance. In the absence of viscosity, the decreasing radius is associated with an increasing, transversally uniform velocity $v = Q/\pi r_s^2$ and an increasing depression $p = -v^2/2 = -Q^2/2\pi^2 r_s^4$. This depression becomes large compared with the normal stress due to the surface tension ($\approx 1/r_s$) when $r_s \ll Q^{2/3}$, and it is to be balanced by the outward electric stress, which requires $E_n = Q/\pi r_s^2$ at the surface. (This balance is reminiscent of a model of Mestel 1994 for the flow in the meniscus.) On the other hand, the axial field induced at the jet by the surface charge in the cone is $E_x = \partial\varphi_T/\partial R|_{\theta=0} = A/2x^{1/2}$ for $x \gg Q^{2/3}$. Since the surface of the jet should be an equipotential, this field is to be balanced by the field of the charge distribution at the surface of the jet (where $\sigma = E_n$), which acts as a charged streak leading to the axial field $(\ln\epsilon)\,\mathrm{d}(E_n r_s)/\mathrm{d}x$ to leading order in an expansion containing logarithms of $\epsilon = r_s/x$ (Ashley & Landahl 1965). Thus, in this approximation (i.e. leaving out other logarithmic terms),

$$r_s = \frac{Q/\pi\widetilde{A}}{x^{1/2}}, \quad v = E_n = \frac{\pi\widetilde{A}^2}{Q}x \quad \text{for} \quad x \gg Q^{2/3}, \tag{3.1f}$$

where $\widetilde{A} = A/(-\ln\epsilon)$. These results can be recast in tilde variables simply by setting $Q = 1$.

The electric field required to keep a constant conduction current I in the ever thinning liquid jet is $E_x^i = I/\pi r_s^2 = \pi\widetilde{A}^2(I/Q^2)x$, which should exist when the surface convection current $I_s = 2\pi\sigma r_s v \approx 2\widetilde{A}^3 x^{3/2}/Q$ is small compared with I. The condition used above, that the surface of the jet is an equipotential from the point of view of the gas, breaks down when E_x^i becomes of the order of $A/2x^{1/2}$, which happens when x is of the order of $x_t = Q^{4/3}/I^{2/3}$, up to logarithms. The electric field in the liquid cannot continue increasing linearly with x when $x = O(x_t)$ and beyond, so that the conduction current can no longer be maintained and has to become a surface convection current. An order of magnitude estimate of the total current can be obtained from the condition that $I_s = O(I)$ when $x = O(x_t)$, which, with the estimate of I_s given above in this paragraph, yields $I = O(Q^{1/2})$. The transfer of bulk current to surface current occurs at non-dimensional distances of order $x_t = Q$ downstream of the cone-to-jet transition region, where the non-dimensional radius of the jet is $r_s = O(Q^{1/2})$, the non-dimensional velocity and surface charge density are of order unity, and the non-dimensional axial field is of order $Q^{-1/2}$. These results provide a physical interpretation for the scales postulated by Gañán-Calvo (1997) (see also the experimental results in Gañán-Calvo 1999). It is also in the region of $x = O(Q)$ where, if $Re = O(1)$, viscous forces begin to affect the whole cross-section of the jet and the electric shear at the surface begins to accelerate the flow. This is because $Re^{-1}\nabla^2\boldsymbol{v} \approx Re^{-1}r^{-1}\partial(r\partial\boldsymbol{v}/\partial r)/\partial r$ is of the same order as $\boldsymbol{v}\cdot\nabla\boldsymbol{v}$ (both are of order

https://doi.org/10.1017/S0022112003004385 Published online by Cambridge University Press

Q^{-1}), and because σE_t is of the same order as $Re^{-1}\partial v/\partial r$ (both are of order $Q^{-1/2}$). The effect of the surface tension is negligible in this region.

Further downstream, for $x \gg Q$, most of the electric current is due to convection of surface charge; the axial electric field is dominated by the contribution of the cone: $E_x = A/2x^{1/2}$; and the electric shear continues to accelerate the liquid, whose velocity is nearly uniform across the jet and whose pressure is nearly uniform (because $p = O[\max(E_n^2, 1/r_s)] \ll v^2$, assuming the results below). In these conditions,

$$\pi r_s^2 v = Q, \quad 2\pi r_s v\sigma = I, \quad \frac{\mathrm{d}}{\mathrm{d}x}\left(\pi r_s^2 v^2\right) = 2\pi r_s \sigma E_x, \tag{3.2}$$

expressing the conservation of mass, charge and momentum in the jet. These equations can be solved to yield

$$\left.\begin{aligned} r_s &= \frac{r_{s_0}}{[1+8\pi A(I/Q^3)r_{s_0}^4 x^{1/2}]^{1/4}} \sim \left(\frac{Q^3}{8\pi A I}\right)^{1/4} \frac{1}{x^{1/8}}, \\ v &= \frac{q}{\pi r_s^2} \sim \left(\frac{8A}{\pi}\frac{I}{Q}\right)^{1/2} x^{1/4}, \quad \sigma = \frac{I\, r_s}{2Q} \sim \left(\frac{I^3}{128\,\pi A\, Q}\right)^{1/4} \frac{1}{x^{1/8}}, \end{aligned}\right\} \tag{3.3}$$

where $r_{s_0} = O(Q^{1/2})$ is a constant.

Using these results, the surface tension can be seen to come back into play ($1/r_s = O(E_n^2)$ with $E_n = \sigma$) when $x = O(I^{5/6}Q^{1/4}) = O(Q^{7/3})$. Even further downstream, the normal electric stress becomes negligible and condition (2.7*a*) at the surface reduces to the balance of surface tension and pressure. This, however, does not affect (3.3), which coincide with the downstream asymptotics of Gañán-Calvo (1997) for any $x \gg Q$.

3.3. *Additional comments*

The electric charge of the jet in the region $Q^{2/3} \ll x \ll Q$ induces an electric field at the meniscus which is only logarithmically small compared with the field of a Taylor cone. The boundary conditions (3.1*d–f*) are thus correct only to leading order in an expansion in powers of $1/\ln Q$ and, since this is not a small parameter for any realistic value of Q, the solution of problem (3.1) cannot provide an accurate asymptotic description of the transition region. Equations (3.1) are best used as order of magnitude balances, as has been done in the preceding section. A qualitative estimate of the effect of the electric charge of the jet on the shape of the meniscus for $Q^{2/3} \ll (-x) \ll Q$ can be obtained in this vein by treating $\epsilon = r_s/x$ as a small constant. (Actually the results that follow can be derived without the condition that ϵ be a constant. They are the leading term of a formal expansion in both powers and logarithms of R, of the type introduced by Glauert & Lighthill (1955) for a different problem. The next term of the expansion, however, is only logarithmically smaller than the leading term. The reader is referred to the original paper for details.) The electric potential satisfying the condition $\varphi = 0$ at the surface of the jet is then $\varphi = A_0 R^{1/2}[P_{1/2}(\cos\theta) + Q_{1/2}(\cos\theta)/\ln\epsilon]$, where $Q_{1/2}$ is Legendre's function of the second kind. Proceeding as in Fernández de la Mora (1992), the condition $\varphi = 0$ at the meniscus gives the new angle of the cone as $\alpha + \delta(\epsilon)$, with $\delta(\epsilon) = -[Q_{1/2}(-\cos\alpha)/\sin\alpha\, P'_{1/2}(-\cos\alpha)]/\ln\epsilon \approx 1.3887/\ln\epsilon < 0$, while the equilibrium of normal stresses far upstream gives $A_0 = A[1 + O(1/\ln\epsilon)]$. This result could explain the reduction of the angle of the cone that is observed experimentally at high flow rates. The meniscus becomes a Taylor cone only when the effect of the jet becomes small, for $x \gg Q$, provided the influence of the finite sizes of the capillary and the

https://doi.org/10.1017/S0022112003004385 Published online by Cambridge University Press

jet is still negligible. The small parameter $1/\ln\epsilon$ was anticipated and widely used by Gañán-Calvo (1997).

The qualitative description of the asymptotic solution for $Q \to \infty$ in § 3.2 is apparently consistent and complete, and predicts an electric current proportional to $Q^{1/2}$ and independent of β. It is now appropriate to ascertain the range of β in which this solution can be realized. Under the assumption of fast surface charge relaxation that has been used, $\sigma = E_n$ and the surface current is $I_s = 2\pi r_s v_s \sigma = O(x^{3/2}/Q)$ for $Q^{2/3} \lesssim x \lesssim Q$. The normal electric field at the liquid side of the surface required to supply this current is, from (2.7*c*), $E_n^i = r_s^{-1}\mathrm{d}(I_s/2\pi)/\mathrm{d}x = O(x/Q^2)$, while $E_n = O(x/Q)$ in the gas. The surface charge will be screening the liquid when $\beta E_n^i \ll E_n$, which amounts to $Q \gg \beta$, a condition already found in the analysis of the transition region. This condition imposes a high lower bound on the flow rate for polar liquids (β large). If it is not satisfied, then the assumption of fast charge relaxation fails simultaneously in the whole length between the transition region and the bulk-to-surface current transfer region $x = O(Q)$.

The numerical solutions of § 3.1 and the experimental results in the literature show that the cone–jet regime extends to fairly small values of Q/β before giving way to other, non-stationary regimes. It is of interest to investigate how these regimes may come about when $\beta \gg Q \gg 1$. In these conditions, charge relaxation is still possible far upstream in the cone, where the surface current is small compared with the bulk current and conservation of mass and electric current require $v = O(Q/R^2)$ and $E_R^i = O(I/R^2)$. In this far region $\sigma = E_n = -R^{-1}\partial\varphi_T/\partial\theta = O(R^{-1/2})$, leading to $I_s = O(Q/R^{3/2})$ and to $E_n^i = O(Q/R^{7/2})$ (via (2.7*c*)). The condition $\beta E_n^i \ll E_n$ breaks down when R is of order $R_e = (\beta Q)^{1/3}$, where $E^i = O(\beta^{-7/6}Q^{-1/6})$ and the bulk and surface currents are both of order $(Q/\beta)^{1/2}$, which is the order-of-magnitude estimate proposed by Fernández de la Mora & Loscertales (1994). The residence time becomes small compared with the electric relaxation time when $R \ll R_e$. Then the surface charge density cannot keep pace with the increasing normal field and becomes negligible in (2.7*d*), which reduces to $E_n^i \approx E_n/\beta$. The electric field in the liquid is as large as it can possibly be here, but it is still small compared with the electric field in the gas when $\beta \gg 1$, so that the surface of the liquid is still an equipotential from the point of view of the gas. The normal electric stress is still $\approx E_n^2/2$ due to the polarization charge, though the surface density of free charge is negligible. Under these conditions, the flow in the meniscus for $R \ll R_e$ and down to the region of $R = O(Q^{2/3})$ may be as in the preceding section. Once the liquid reaches the slender jet, however, the normal electric stress of order x^2/Q^2 that would be required to prevent the collapse of the surface under the depression created by the stationary motion of the liquid ceases to be available, because the electric field normal to the jet is induced by the free surface charge, which is too small, not by the outer field (but see § 3.5). This description suggests that a pulsating regime akin to the microdripping regime (Cloupeau & Prunet-Foch 1990, 1994) could be established, with a stationary conical meniscus followed by a transient region of size $Q^{2/3}$ or smaller whose rounded surface is periodically disrupted to shed blobs of liquid.

3.4. *Estimations for small flow rates*

A possible structure of the solution in the asymptotic limit $Q \to 0$ with $(\beta, Re) = O(1)$ is discussed here for completeness. Such a solution, if it exists, is not realized experimentally because the actual flow becomes time-dependent before the flow rate can be decreased arbitrarily. However, the asymptotic estimates that follow could still reveal some features of the real solution and perhaps provide insight into the

https://doi.org/10.1017/S0022112003004385 Published online by Cambridge University Press

cause of the transition to a non-stationary regime. A limitation of the model problem of § 2 in the range of small values of Q may arise from the assumption of a constant electrical conductivity. When the conductivity of the liquid is due to a strong electrolyte, Fernández de la Mora & Loscertales (1994) showed that a sheath layer of reduced ion concentration and conductivity appears around the surface and increases in thickness when the ratio of the residence time to the electric relaxation time decreases, which happens when Q decreases. It could be argued that ignoring this layer may result in an artificially extended range of flow rates for which a solution exists. In fact, some of the numerical solutions of § 3.1 are for values of Q smaller than the experimental minimum. However, the sheath layer seems to be always thin, and its real importance, as well as the cause of the minimum experimental flow rate, are still to be ascertained.

Leaving this effect aside, the numerical results show that the electric current approaches zero and the rear end of the recirculation bubble approaches the apex of the cone when Q decreases. The upstream conditions (2.11) and (2.12) require that: $E = O(1/R^{1/2})$ in the gas, for the normal electric stress to balance surface tension; $E^i = O(I/R^2)$ in the liquid, to keep a constant conduction current; and $v = O(IRe/R^{3/2})$ in the slow, viscosity-dominated flow in the Taylor cone, from the viscous–electric shear balance $Re^{-1}v/R \sim \sigma E_t$ (with $\sigma \approx E_n$ when $E \gg E^i$). More detailed accounts of this flow have been given by Barrero *et al.* (1999) and Cherney (1999*a*, *b*). To leading order, its stream function is given by the first term of ψ in (2.12). The flow is forward, toward the apex, near the surface and backward near the symmetry axis. It carries a surface current $I_s = O(\sigma vR) = O(IRe/R)$ which becomes of the order of the total current I for $R = O(Re)$. At these distances from the apex the pressure and viscous stress of the liquid on the surface are of order $Re^{-1}v/R = O(I/Re^{5/2})$, too small to upset the surface tension–normal electric stress balance when $I \ll 1$, and the electric field in the liquid is $E^i = O(I/Re^2)$, small compared with the electric field in the gas. In these conditions, since most of the electric current is transferred to the surface in the region of $R = O(Re)$, the following order-of-magnitude balances should hold for $R \ll Re$:

$$\sigma vR \sim I, \quad E_n^2 \sim \frac{1}{R}, \quad \frac{1}{Re}\frac{v}{R} \sim \sigma E_t, \quad \sigma \approx E_n, \tag{3.4}$$

expressing the conservation of the electric current, the equilibrium of stresses normal and tangent to the surface, and condition (2.7*d*) with βE_n^i neglected, respectively. These balances give

$$v = O\left(\frac{I}{R^{1/2}}\right), \quad \sigma \approx E_n = O\left(\frac{1}{R^{1/2}}\right), \quad E_t = O\left(\frac{I}{ReR}\right). \tag{3.5}$$

The residence time $R/v = O(R^{3/2}/I)$ becomes of the order of the electric relaxation time (of order unity when $\beta = O(1)$) for $R = O(I^{2/3})$, but this does not affect the balances (3.4) because no current is being transferred to the surface. The estimates (3.5) can be used for $R \ll I^{2/3}$. The pressure and viscous stress increase as $I/ReR^{3/2}$ when R decreases. They become of the order of the surface tension and normal electric stress (of $O(1/R)$) and begin to deform the surface when $R = O(I^2/Re^2)$, which defines the characteristic size of the cone-to-jet transition region. In this region $v = O(Re)$ and σ, E_n and E_t are all of order Re/I. The order of the flow rate for a given small I can be determined from the condition that a substantial part of the flow in the transition region should not recirculate if a stationary jet is to be formed. Thus $Q = O(vR^2) = O(I^4/Re^3)$. The inertia of the liquid is negligible in the transition

https://doi.org/10.1017/S0022112003004385 Published online by Cambridge University Press

region because $(v^2/R)/(v/ReR^2) = O(I^2) \ll 1$. The inertia should remain negligible in the leading part of the jet, for $x \gg I^2/Re^2$, where the electric shear acting on the surface is to be balanced by a streamwise variation of the pressure rather than by an acceleration of the liquid. In this region of the jet,

$$vr_s^2 \sim Q, \quad \sigma v r_s \sim I, \quad p \sim \frac{1}{r_s}, \quad \frac{p\, r_s^2}{x} \sim \sigma E_t r_s, \quad E_t \sim \frac{1}{x^{1/2}}, \tag{3.6}$$

expressing the conservation of mass and electric current, the balance of pressure and surface tension at the surface, the x-momentum equation integrated across the jet (effectively $\mathrm{d}(\pi r_s^2 p)/\mathrm{d}x \approx 2\pi r_s \sigma E_t$), and the fact that the axial electric field is dominated by the contribution of the electric charge at the surface of the cone. From these order-of-magnitude balances,

$$r_s = O\left(\frac{Q}{Ix^{1/2}}\right), \quad v = O\left(\frac{I^2 x}{Q}\right), \quad \sigma = O\left(\frac{1}{x^{1/2}}\right), \quad p = O\left(\frac{Ix^{1/2}}{Q}\right), \tag{3.7}$$

which were first derived by Cherney (1999*b*). The ratio $v^2/p = O(I^3 x^{3/2}/Q)$ becomes of order unity, and the inertia of the liquid comes into play in the integrated momentum equation, when $x = O(Q^{2/3}/I^2)$. Further downstream, the fourth condition (3.6) should be replaced by the third condition (2.9) and the solution takes the asymptotic form (2.10).

According to the estimates calculated in this section, the electric current is essentially the surface convection current in the region of the cone $Re \gg R \gg I^2/Re^2$ where (3.5) holds, but the capability of the bulk–surface charge exchange to rapidly modify the distribution of surface charge in response to a perturbation that lets the electric field enter the liquid is lost for $R \ll I^{2/3}$. The existence of a solution of the type described here depends on the assumption that the flow can negotiate the region $I^{2/3} \gg R \gg I^2/Re^2$, which is not obvious. The pseudotransient numerical method that has been used cannot follow a real transient, but it first fails to converge immediately upstream of the transition region when Q is decreased.

3.5. *Creeping flow*

The Reynolds number defined in (2.8) is small for a number of liquids of high viscosity or high electrical conductivity used in some experiments, for example in the experiments carried out by Fernández de la Mora & Loscertales (1994) with ethylene glycol and triethylene glycol. The limiting form of the solution of the problem formulated in §2 for $Re \to 0$ is therefore of interest. A limiting problem can be obtained by introducing the rescaled variables ($\boldsymbol{x}/Re$, $\boldsymbol{v}/Re$, $Re\, p$, $Re^{1/2}\sigma$, $\varphi^i/Re^{1/2}$, $\varphi/Re^{1/2}$, Q/Re^3, $I/Re^{3/2}$) into (2.5)–(2.7) and (2.11)–(2.12) and then letting $Re \to 0$. This amounts to replacing the original scaling factors (2.4) by

$$\left.\begin{gathered} Q_0' = \frac{\epsilon_0^2 \gamma^3}{\mu^3 K^2}, \quad R_0' = \frac{\epsilon_0 \gamma}{\mu K}, \quad v_0' = \frac{\gamma}{\mu}, \\ E_0' = \frac{\mu^{1/2} K^{1/2}}{\epsilon_0}, \quad I_0' = \frac{\epsilon_0 \gamma^2}{\mu^{3/2} K^{1/2}}, \quad \varphi_0' = E_0' R_0', \quad \sigma_0' = \epsilon_0 E_0', \end{gathered}\right\} \tag{3.8}$$

which can be obtained from balances similar to those that led to (2.4) except that now the inertia of the liquid is not important and $\Delta p = O(\mu v_0'/R_0')$. The limiting problem differs from the original problem in that: (i) the convective acceleration $\boldsymbol{v}\cdot\nabla\boldsymbol{v}$ disappears from the left-hand side of (2.5*b*); (ii) the factor Re changes to unity in this equation, in (2.12) and in the expression of the viscous stress tensor; and (iii) the

https://doi.org/10.1017/S0022112003004385 Published online by Cambridge University Press

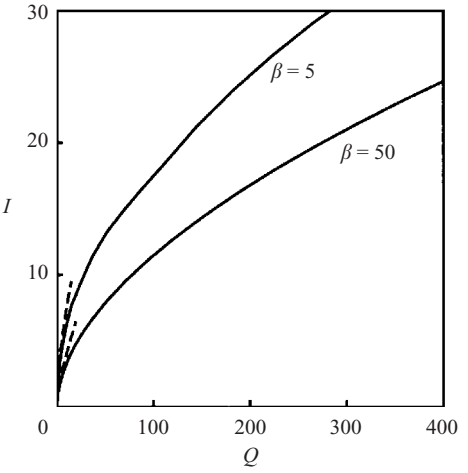


FIGURE 6. Electric current as a function of the flow rate for $\beta = 5$ and 50 in the absence of fluid inertia ($Re = 0$). The dashed curves are the results of figure 5(a) for $Re = 1$, which are repeated here for comparison.

downstream boundary conditions (2.10) change to (3.7), which follow from (3.6) when the electric shear is balanced by a pressure rise rather than by an acceleration of the jet. In the remainder of this section the rescaled variables will be denoted with the same symbols as used before for the original non-dimensional variables. The limiting problem contains the two non-dimensional parameters Q and β.

The rescaled electric current I computed numerically is plotted in figure 6 as a function of the rescaled flow rate Q for two values of β. As in the general case, the electric current increases nearly as the square root of the flow rate. The curve of figure 6 for $\beta = 50$ is indistinguishable from a parabola for Q greater than about 10, but the value of $I/Q^{1/2}$ is less than a half of the experimental value of Fernández de la Mora & Loscertales (1994). The discrepancy is due to the inertia of the liquid. In fact, it is not Re alone, but also the flow rate, that determine the influence of the inertia in a given experiment. It should also be noticed that the largest values of Q in figure 6 correspond typically to dimensional flow rates far smaller than in real experiments, because the scaling factor Q_0' in (3.8) is extremely small.

The asymptotic estimates of § 3.2 for large flow rates need be revised in the absence of inertia. The characteristic size of the region where the liquid surface departs from a cone is now $R_c = Q^{1/2}$, and the characteristic values of the velocity of the liquid and the electric field of the gas in this region are $v_c = 1$ and $E_c = Q^{-1/4}$. These modified estimates follow from the condition that the characteristic velocity $v_c = Q/R_c^2$ should originate normal viscous stresses and pressure variations (of order $v_c/R_c = Q/R_c^3$) sufficiently strong to upset the balance of normal electric stress and surface tension (both of order $1/R_c$). Further estimates along the lines of § 3.2 show that, when $Q \gg \beta^2$ (the case $1 \ll Q \ll \beta^2$ will be discussed below): (i) the surface convection current is small compared with the bulk conduction current in this region; (ii) the surface charge screens the liquid because the residence time is large compared with the electric relaxation time; and (iii) the surface is nearly an equipotential and the electric shear is small compared with the normal stress, so that the liquid is pushed into the jet by a local depression rather than by the electric shear.

https://doi.org/10.1017/S0022112003004385 Published online by Cambridge University Press

In the jet, of radius $r_s(x) \ll Q^{1/2}$, the velocity is $v \approx Q/\pi r_s^2$. The streamwise variation of this velocity leads to radial viscous stresses of order v/x (because $\partial v_r/\partial r = O(\partial v/\partial x)$ from the continuity equation), which is also the order of the axial pressure variations (from the momentum equation integrated across the jet). The balance of these stresses and the normal electric stress at the surface requires $E_n^2 = O(v/x)$, whence $E_n = O(Q^{1/2}/x^{1/2}r_s)$. On the other hand, taking $\sigma \approx E_n$, the condition that the surface convection current ($I_s = 2\pi\sigma r_s v$) and the bulk conduction current ($I_b = \pi r_s^2 E_x^i$) be of the same order, with $E_x^i = O(1/x^{1/2})$ due to the surface charge of the cone, is satisfied for r_s of the order of $r_{s_t} = Q^{3/8}$, which corresponds to the bulk-to-surface current transfer region. At variance with the results of § 3.2, this region is not much longer than the region discussed in the preceding paragraph. This is a consequence of the condition introduced in § 3.2, that the axial field induced by the charge of the jet should balance the field of the cone – of $O(1/x^{1/2})$ – in the leading region of the jet where conduction in the bulk dominates surface convection. The axial field associated with E_n above is of order $\ln(r_s/x)\,\mathrm{d}(E_n r_s)/\mathrm{d}x = O[\ln(r_s/x)\,Q^{1/2}/x^{3/2}]$, because the jet acts as a line charge. The condition that this field should be of $O(1/x^{1/2})$ gives r_s/x decreasing exponentially with $x/Q^{1/2}$ from $r_s = O(Q^{1/2})$ in the non-slender region of the preceding paragraph to $r_s = O(Q^{3/8})$ in the bulk-to-surface current transfer region of the jet. It is therefore appropriate to take $x = O(Q^{1/2})$ in both regions, up to factors of order $\ln Q$. In the bulk-to-surface current transfer region, using the estimate of r_s above, $v = O(Q^{1/4})$, $p = O(1/Q^{1/4})$, $E_n = O(1/Q^{1/8})$, and $E_x = O(1/Q^{1/4})$, while the order of magnitude of I_s and I_b is $I = O(Q^{1/2})$. It is also in this region that the electric shear σE_t begins to have importance and to increase the pressure of the liquid, because $p\,r_s^2 \sim \sigma E_t r_s x$, both being of order $Q^{1/2}$. The effect of the surface tension is still formally small. It comes back into play for $x = O(Q)$, after a region where the electric shear-induced pressure variation and the normal viscous stress balance each other and lead to $r_s = O(Q^{3/4}/x^{3/4})$. The final asymptotic regime described by (3.7) is attained for $x \gg Q$.

The estimates above rely on the assumption that the free charge at the surface of the jet is screening the liquid from the outer axial field in the region where the radius decreases from $r_s = O(Q^{1/2})$ to $r_s = O(Q^{3/8})$. With $\sigma \approx E_n$ in this region, the normal electric field that is required at the liquid side of the surface in order for conduction to follow the variation of I_s can be estimated via (2.7*c*), as has been done in the second paragraph of § 3.3. The result is now $E_n^i = O(Q^{3/4}/r_s^3)$, and thus $\beta E_n^i/E_n = O(\beta Q^{1/2}/r_s^2)$, where x has been replaced by $Q^{1/2}$ in the estimates at the beginning of the preceding paragraph. The condition $\sigma \approx E_n$ requires that $\beta E_n^i/E_n \ll 1$ for any $r_s \gg r_{s_t}$. This condition is satisfied when $Q \gg \beta^4$, which imposes a lower bound on the flow rate. If $\beta \gg 1$ and $Q \ll \beta^4$, then βE_n^i becomes comparable to E_n when the radius of the jet is still of the order of $r_{s_e} = \beta^{1/2}Q^{1/4} \gg r_{s_t}$, in a region where $I_s = O(Q^{3/4}/\beta)$. The density of free surface charge cannot increase at the pace of E_n beyond this point, and the screening of the liquid depends entirely on the polarization charge at its surface. The cause of the polarization is to be sought in the electric field in the liquid, where $\boldsymbol{\nabla}\cdot\boldsymbol{E}^i = 0$ requires $E_x^i/x \sim E_n^i/r_s$ in orders of magnitude. This condition, along with $\beta E_n^i \approx E_n$, the screening condition $E_n r_s/x \sim E_x \sim 1/x^{1/2}$ (up to logarithms), and the stress-balance condition $v/x \sim E_n^2$, give now $x = O(Q^{1/2})$, $E_n = O(Q^{1/4}/r_s)$ and $E_x^i = O(Q^{3/4}/\beta r_s^2)$. The axial field in the liquid, whose streamwise variation causes the radial field E_n^i that polarizes the surface, becomes of the order of the axial field $E_x = O(Q^{-1/4})$ induced by the charge of the meniscus when $r_s = O(Q^{1/2}/\beta^{1/2})$, in a region where $(I_b, I_s) = O(Q^{3/4}/\beta)$. The screening condition need not be satisfied further downstream, where $E_x^i \approx E_x = O(1/x^{1/2})$ (for $x \gg Q^{1/2}$). Carrying this axial

https://doi.org/10.1017/S0022112003004385 Published online by Cambridge University Press

field to $\nabla \cdot \boldsymbol{E}^i = 0$ gives $E_n \approx \beta E_n^i = O(\beta r_s/x^{3/2})$. In addition, the last term of (2.7a) comes to dominate the normal electric stress, so that the stress balance condition changes to $v/x \sim \beta E_t^2$. The density of free surface charge estimated from the condition of conservation of the current is $\sigma = O(I/r_s v) = O(r_s/\beta Q^{1/4})$ (using $I = O(Q^{3/4}/\beta)$). It becomes of the order of E_n when $x = O(\beta^{4/3} Q^{1/6})$. This is followed by another region where, under the action of the electric shear, the pressure and normal viscous stress become much larger than the normal electric stress and balance each other, as in the analogue region of the case $Q \gg \beta^4$ discussed before. The balance $v/x \sim \sigma E_x x/r_s$ yields $r_s = O(\beta^{1/2} Q^{5/8}/x^{3/4})$, which applies until surface tension comes back into play, at $x = O(Q^{3/2}/\beta^2)$, and the solution enters the asymptotic regime (3.7).

The value $r_{s_e} = \beta^{1/2} Q^{1/4}$ of the characteristic radius of the jet for which $\beta E_n^i/E_n = O(1)$ and the characteristic size $R_c = Q^{1/2}$ of the non-slender region where the surface departs from a cone coincide when $Q = \beta^2$. When $1 \ll Q \ll \beta^2$, electric relaxation has already ceased to be effective in the meniscus, at distances from the apex of order $R_e = (\beta Q)^{1/3} \gg R_c$, where the free surface charge fails to screen the liquid and the current freezes at $I = O(Q^{1/2}/\beta^{1/2})$. These are the scales of the relaxation region and the electric current derived by Fernández de la Mora & Loscertales (1994), which have been discussed in the last paragraph of § 3.3. In the absence of electric relaxation, the polarization charge must take over in the rest of the meniscus, for $R \ll R_e$, and in the jet. The estimates of the preceding paragraph apply in the jet also for this case. The only differences arise beyond the region of $r_s = O(Q^{1/2}/\beta^{1/2})$ where the axial field induced by the cone first enters the jet. Now the effect of the surface tension begins to be important for $x = O(\beta^{1/2} Q^{1/2})$. Surface tension takes care of the pressure and normal viscous stress in a region that extends from these distances to $x = O(\beta Q^{1/3})$, where the density of free surface charge finally becomes of the order of E_n and the electric shear begins to have importance. The asymptotic regime (3.7) is obtained for $x \gg \beta Q^{1/3}$.

4. Conclusions

The cone-to-jet transition region of an electrospray operating in the cone–jet mode has been studied numerically and asymptotically. When this transition region is small compared with the size of the meniscus and the length of the jet, the local flow and the electric current depend only on the flow rate non-dimensionalized with $\epsilon_0 \gamma/\rho K$ and the two non-dimensional parameters (2.8), which are properties of the liquid. The surface of the liquid tends to a Taylor cone upstream of the transition region and to a slowly varying jet downstream of the transition region.

Numerical computations of the local flow show a recirculation bubble in the transition region that recedes toward the cone when the non-dimensional flow rate is increased. The electric current carried by the jet increases monotonically with the flow rate.

The asymptotic structure of the solution for large values of the non-dimensional flow rate Q consists of an inviscid region of characteristic size proportional to $Q^{2/3}$, where the surface of the liquid is almost equipotential and the electric current is dominated by conduction in the bulk, followed by a slender region of length and width proportional to Q and $Q^{1/2}$, respectively, where the bulk conduction current becomes a surface convection current and the electric shear acting on the charged surface is transmitted by viscosity to the whole cross-section of the jet and begins to accelerate the liquid. The electric current in this asymptotic regime increases proportionally to $Q^{1/2}$ and is independent of the dielectric constant of the liquid.

https://doi.org/10.1017/S0022112003004385 Published online by Cambridge University Press

Conditions of applicability of these asymptotic results to liquids with large dielectric constants are discussed qualitatively. A modified asymptotic structure of the flow in the absence of fluid inertia suggests that the electric current is proportional to the square root of the flow rate also in this case.

I am indebted to Professors A. Barrero and J. Fernández de la Mora for introducing me to this problem and for their advice and ideas. Useful discussions with Professors A. M. Gañán-Calvo and I. G. Loscertales are also gratefully acknowledged. This work was supported by the Spanish Ministerio de Ciencia y Tecnología project BFM2001-3860-C02-02.

REFERENCES

Ashley, H. & Landahl, M. 1965 *Aerodynamics of Wings and Bodies*, Chap. 6. Addison-Wesley.

Bailey, A. G. 1988 *Electrostatic Spraying of Liquids*. Wiley.

Barrero, A., Gañán-Calvo, A. M., Dávila, J., Palacios, A. & Gómez-González, E. 1999 The role of the electrical conductivity and viscosity on the motions inside Taylor cones. *J. Electrostatics* **47**, 13–26.

Chen, D.-R. & Pui, D. Y. H. 1997 Experimental investigation of scaling laws for electrospraying: dielectric constant effect. *Aerosol Sci. Technol.* **27**, 367–380.

Chen, D.-R., Pui, D. Y. H. & Kaufman, L. 1995 Electrospraying of conducting liquids for monodisperse aerosol generation in the 4 nm to 1.8 μm diameter range. *J. Aerosol Sci.* **26**, 963–977.

Cherney, L. T. 1999*a* Structure of Taylor cone–jets: limit of low flow rates. *J. Fluid Mech.* **378**, 167–196.

Cherney, L. T. 1999*b* Electrohydrodynamics of electrified liquid menisci and emitted jets. *J. Aerosol Sci.* **30**, 851–862.

Cloupeau, M. & Prunet-Foch, B. 1989 Electrostatic spraying of liquids in cone–jet mode. *J. Electrostatics* **22**, 135–159.

Cloupeau, M. & Prunet-Foch, B. 1990 Electrostatic spraying of liquids. Main functioning modes. *J. Electrostatics* **23**, 165–184.

Cloupeau, M. & Prunet-Foch, B. 1994 Electrohydrodynamic spraying functioning modes: a critical review. *J. Aerosol Sci.* **25**, 1021–1036.

Fenn, J. B., Mann, M., Meng, C. K., Wong, S. K. & Whitehouse, C. 1989 Electrospray ionization for mass spectrometry of large biomolecules. *Science* **246**, 64–71.

Fernández de la Mora, J. 1992 The effect of charge emission from electrified liquid cones. *J. Fluid Mech.* **243**, 561–573.

Fernández de la Mora, J. & Loscertales, I. G. 1994 The current emitted by highly conducting Taylor cones. *J. Fluid Mech.* **260**, 155–184.

Fernández de la Mora, J., Navascués, J., Fernández, F. & Rosell-Llompart, J. 1990 Generation of submicron monodisperse aerosols in electrosprays. *J. Aerosol Sci.* **21**, suppl. S673–S676.

Fernández-Feria, R., Fernández de la Mora, J. Pérez-Saborid, M. & Barrero, A. 1999 Conically similar swirling flows at high Reynolds numbers. *Q. J. Mech. Appl. Maths.* **52**, 1–53.

Gamero-Castaño, M. & Hruby, V. 2002 Electric measurements of charged sprays emitted by cone–jets. *J. Fluid Mech.* **459**, 245–276.

Gañán-Calvo, A. M. 1997 Cone–jet analytical extension of Taylor's electrostatic solution and the asymptotic universal scaling laws in electrospraying. *Phys. Rev. Lett.* **79**, 217–220.

Gañán-Calvo, A. M. 1999 The surface charge in electrostatic spraying: its nature and its universal scaling laws. *J. Aerosol Sci.* **30**, 863–872.

Gañán-Calvo, A. M., Dávila, J. & Barrero, A. 1994*a* The emitted current and droplet size laws in steady cone–jet electrosprays of polar and nonpolar liquids. *Proc. 4th Intl Aerosol Conf.* (ed. R. C. Flagan), pp. 44–46. American Association for Aerosol Research.

https://doi.org/10.1017/S0022112003004385 Published online by Cambridge University Press

Gañán-Calvo, A. M., Dávila, J. & Barrero, A. 1997 Current and droplet size in the electrospraying of liquids. Scaling laws. *J. Aerosol Sci.* **28**, 249–275.

Gañán-Calvo, A. M., Lasheras, J. C., Dávila, J. & Barrero, A. 1994*b* The electrostatic spray emitted from an electrified conical meniscus. *J. Aerosol Sci.* **25**, 1121–1142.

Glauert, M. B. & Lighthill, M. J. 1955 The axisymmetric boundary layer on a long thin cylinder. *Proc. R. Soc. Lond.* A **230**, 188–203.

Gomez, A. & Tang, K. 1994 Charge and fission of droplets in electrostatic sprays. *Phys. Fluids* **6**, 404–414.

Grace, J. M. & Marijnissen, J. C. M. 1994 A review of liquid atomization by electrical means. *J. Aerosol Sci.* **25**, 1005–1019.

Hartman, R. P. A., Borra, J.-P., Brunner, D. J., Marijnissen, J. C. M. & Scarlett, B. 1999 The evolution of electrohydrodynamic sprays produced in the cone–jet mode, a physical model. *J. Electrostatics* **47**, 143–170.

Hayati, I., Bailey, A. & Tadros, Th. F. 1986 Mechanisms of stable jet formation in electrohydrodynamic atomization. *Nature* **319**, 41–43.

Hayati, I., Bailey, A. & Tadros, Th. F. 1987*a* Investigations into the mechanism of electrohydrodynamic spraying of liquids. I. *J. Colloid Interface Sci.* **117**, 205–221.

Hayati, I., Bailey, A. & Tadros, Th. F. 1987*b* Investigations into the mechanism of electrohydrodynamic spraying of liquids. II. *J. Colloid Interface Sci.* **117**, 222–230.

Jaworek, A. & Krupa, A. 1999 Classification of the modes of EHD spraying. *J. Aerosol Sci.* **30**, 873–893.

Jones, A. R. & Thong, K. C. 1971 The production of charged monodisperse fuel droplets by electrical dispersion. *J. Phys.* D: *Appl. Phys.* **4**, 1159–1166.

Landau, L. D. & Lifshitz, E. M. 1960 *Electrodynamics of Continuous Media*, Chap. 2. Pergamon.

Loscertales, I. G., Barrero, A., Guerrero, I., Cortijo, R., Márquez, M. & Gañán-Calvo, A. M. 2002 Micro/nano encapsulation via electrified coaxial liquid jets. *Science* **295**, 1695–1698.

Martínez-Sánchez, M., Fernández de la Mora, J., Hruby, V., Gamero-Castaño, M. & Khayms, V. 1999 Research on colloidal thrusters. *Proc. 26th Intl Electric Propulsion Conference, Kitakyushu, Japan*, pp. 93–100. Electric Rocket Propulsion Society.

Mestel, A. J. 1994 The electrohydrodynamic cone–jet at high Reynolds number. *J. Aerosol Sci.* **25**, 1037–1047.

Mueller, J. M. 2000 Thruster options for microspacecraft: A review and evaluation of state-of-the-art and emerging technologies. In *Micropropulsion for Small Spacecraft* (ed. M. M. Micci & A. D. Ketsdever), *Prog. Astro. Aero.* **187**, 45–135, AIAA.

Mutoh, M., Kaieda, S. & Kamimura, K. 1979 Convergence and disintegration of liquid jets induced by an electrostatic field. *J. Appl. Phys.* **50**, 3174–3179.

Pantano, C., Gañán-Calvo, A. M. & Barrero, A. 1994 Zeroth-order, electrohydrostatic solution for electrospraying in cone–jet mode. *J. Aerosol Sci.* **25**, 1065–1077.

Rosell-Llompart, J. & Fernández de la Mora, J. 1994 Generation of monodisperse droplets 0.3 to 4 μm in diameter from electrified cone–jets of highly conducting and viscous liquids. *J. Aerosol Sci.* **25**, 1093–1119.

Shtern, V. & Barrero, A. 1994 Striking features of fluid flows in Taylor cones related to electrosprays. *J. Aerosol Sci.* **25**, 1049–1063.

Shtern, V. & Barrero, A. 1995*a* Bifurcation of swirl in liquid cones. *J. Fluid Mech.* **300**, 169–205.

Shtern, V. & Barrero, A. 1995*b* Instability nature of the swirl appearance in liquid cones. *Phys. Rev.* E **52**, 627–635.

Smith, D. P. H. 1986 The electrohydrodynamic atomization of liquids. *IEEE Trans. Ind. Appl.* **IA 22**, 527–535.

Smith, R. D., Loo, J. A., Ogorzalek, R. R., Busman, M. & Usdeth, H. R. 1991 Principles and practice of electrospray ionization mass spectrometry for large polypeptides and proteins. *Mass Spectrom. Rev.* **10**, 359–451.

Tang, K. & Gomez, A. 1994 Generation by electrospray of monodisperse water droplets for targeted drug delivery by inhalation. *J. Aerosol Sci.* **25**, 1237–1249.

Taylor, G. I. 1964 Disintegration of water drops in an electric field. *Proc. R. Soc. Lond.* A **280**, 383–397.

https://doi.org/10.1017/S0022112003004385 Published online by Cambridge University Press

VONNEGUT, B. & NEUBAUER, R. L. 1952 Production of monodisperse liquid particles by electrical atomization. *J. Colloid Sci.* **7**, 616–623.

ZELENY, J. 1914 The electrical discharge from liquid points, and a hydrostatic method of measuring the electric intensity at their surfaces. *Phys. Rev.* **3**, 69–91.

ZELENY, J. 1915 On the conditions of instability of electrified drops, with applications to the electrical discharge from liquid points. *Proc. Camb. Phil. Soc.* **18**, 71–83.

ZELENY, J. 1917 Instability of electrified liquid surfaces. *Phys. Rev.* **10**, 1–6.

https://doi.org/10.1017/S0022112003004385 Published online by Cambridge University Press